Importance of peakedness in sea surface slope measurements and applications

B. Chapron and V. Kerbaol
Département d'Océanographie Spatiale, Institut Français du Pétrole, Plouzané, France

D. Vandemark
Laboratory for Hydrospheric Processes, NASA Goddard Space Flight Center, Wallops Island, Virginia

T. Elfouhaily
Applied Physics Laboratory, Johns Hopkins University, Laurel, Maryland

Abstract. We recall the simple statistical concept that non-Gaussian distribution peakedness results from the compounding of random processes. This idea is applied to observations and analysis of sea surface slopes as inferred using optical and microwave-scattering measurements. Our study emphasizes the importance of identifying and quantifying the distribution variance and kurtosis from observations. Data are shown to indicate consistently non-Gaussian peakedness, to indicate the need to report at least two parameters in an even order analysis, and to indicate near equivalence between radar and optical data. Physical interpretation for observed infrequent steep slopes is given via compounding statistical processes where normally distributed short-scale waves are modulated because of random fluctuations mainly associated with the underlying long wave field. Implications of non-Gaussian peakedness are provided for altimeter backscatter theory and for modeling wave-breaking probability.

1. Introduction

Ocean surface remote sensing studies often focus on signal backscatter or emission linked to changes in the spectral density of gravity-capillary ocean wavelets. However, it is increasingly apparent that a precise surface slope description for short gravity and gravity-capillary waves is also a vital component in the robust sea surface model needed to assimilate varied satellite and airborne remote sensing data sets. For the example cases of the satellite radar altimeter and scatterometer the sea surface slope probability distribution function (pdf) enters in the direct prediction of the nadir incidence backscatter strength and in the ensemble average implied in standard composite surface scattering models [e.g., *Valenzuela*, 1978], respectively.

In most previous studies that utilize a surface model to address ocean remote sensing data, Gaussian statistics are assumed to describe the surface slope. This first-order approximation is numerically attractive and requires only the variance for a complete model. However, as new and differing satellite sensors come on-line, the requirements for intercomparison and cross validation necessitates physical models with higher precision. The physical motivation to consider a non-Gaussian slope description is well known. A random sea surface may be represented approximately as the sum of independent components. However, the phase between these different wave elevation and/or slope components may locally exhibit correlations due to local strong nonlinear interactions. This modifies distribution Gaussianity. In particular, measurements indicate that the short wave amplitudes will vary over the phase of longer waves, clearly demonstrating the need to go beyond a second-order statistical description [e.g., *Longuet-Higgins*, 1963, 1982]. The capillary-gravity waves that primarily govern the sea surface slope variance and microwave backscatter measurements are superimposed on a continuum of longer waves. These longer waves are also random and travel in various directions. They may also affect the local wind speed near the sea surface. Thus, even without invoking local wave breaking enhancements and simply following linear modulation transfer functions, the capillary-gravity height and slope variances must be considered as random variables: the randomness will result from the randomness of the modulating random variable, i.e., in this discussion, the long wave steepness. Proper treatment of the ocean surface statistical description then requires the use of an advanced stochastic development. As a first step, the known and clearly observed wave nonstationarity in both time and space can be formally introduced to generate higher-order moments in surface slope statistics.

In several publications devoted to non-Gaussian slope statistical descriptions, cumulant expansions such as the Gram-Charlier have been used to describe ocean slope distributions [e.g., *Cox and Munk*, 1954; *Shaw and Churnside*, 1997]. Under such a statistical description the introduction of higher-order correction terms can be difficult to interpret physically. In this paper we develop an analytical surface slope model by adopting the theory of the surface as a compound process. This framework can potentially encompass all sources of nonstationarity such as nonlinear long wave–short wave interactions and/or wind input intermittencies. For such a model, deviation from a Gaussian distribution is directly associated with the strength of the scale variability. The concept of a compound model is often used in a two-scale sense to describe the influ-

Paper number 2000JC900079.
0148-0227/00/2000JC900079$09.00

ence of larger-scale inhomogeneities modulating a dense, normally distributed population of smaller scales [e.g., *Valenzuela*, 1978]. This view seems to be applicable for the random sea surface which visually exhibits groupiness and intermittent characteristics.

This paper presents such a compound model concept. Next, a reevaluation of the Cox and Munk optical measurements and analysis is presented to relate their results to this new formulation. This paper will focus not on the directionality of the slope distribution but rather on its "peakedness" as found in higher-order coefficients of Cox and Munk's fitting procedure and also in their overall pdf normalization based on a blanket increase factor to account for unmeasured steep waves.

A primary finding will be that the known level of pdf departure from Gaussianity is not negligible in many cases and that attempts to invert this information under a compound process assumption may prove useful. Discussion is provided to relate the described pdf to modeled wave breaking. It is postulated that the interactions between scales may provide a breaking wave indicator and that closer examination of the slope peakedness characteristics may lead to estimation of the probability of wave breaking.

Implications of the proposed analysis are then discussed using the near-nadir backscatter measurements of airborne and satellite altimeters to examine the quantitative impact of slope model assumptions. The microwave altimeter is a focus here because of the nearly direct link between slope measurements and near-vertical backscatter under a specular point scattering model. The nadir incidence satellite altimeter backscatter measurement will be inversely proportional to the value of the slope variance; for recent near-nadir airborne radar altimeter measurements it is the measure of the slope pdf shape versus incidence angle that is important [*Jackson et al.*, 1992; *Vandemark et al.*, 1997; *Walsh et al.*, 1998]. Some discrepancies in these reported observations are discussed within the context of our non-Gaussian slope model and the notion of compound surface processes.

2. A Compound Process Model for Surface Slope

For an isotropic sea the Gaussian slope pdf can be expressed as

$$P(s_x, s_y) = P(\mathbf{s}) = \frac{\alpha}{\pi} e^{-\alpha s^2}, \tag{1}$$

where α is the inverse of the total slope variance and s is the modulus of the surface slope vector $\mathbf{s}$ with two perpendicular slope components s_x and s_y. As defined, the pdf is omnidirectional and has the following property:

$$\int_{-\infty}^{\infty}\int_{-\infty}^{\infty} P(\mathbf{s})\, ds_x\, ds_y = 2\pi \int_0^{\infty} sP(s)\, ds = 1. \tag{2}$$

A compound process statistical model is a known form used to envelop larger-scale inhomogeneities in an overall statistical description. For instance, one can think of the sea surface as a collection of randomly distributed patches. The separation scale chosen for such a description must still leave the small patches with a surface area that encompasses a multitude of wavelets. For instance, we can define a patch as having an extent that is some fraction of the peak wavelength and the extent will generally be of the order of meters. This surface will encompass a dense population of gravity-capillary and short-scale waves. We can then suppose that within the patch scale the sea surface slope pdf is locally Gaussian [e.g., *Gotwols and Thompson*, 1994] but that the slope variance parameter varies randomly from patch to patch. It is not requisite that the within-patch moments be strictly Gaussian, but there are no known measurements of the higher even order moments of the surface slope pdf that are associated solely with only a within-the-patch dimension. Such a short-scale pdf assumption follows a long-standing scattering and surface description theory where a modulation transfer function (MTF) is invoked to describe the variability of the short-scale elevation spectral density (implicit Gaussian assumption) within a given patch as a function of the underlying long wave. The MTF studies [e.g., *Plant*, 1986] are a deterministic parallel to the proposed statistical development, and they invoke the same assumption at the short scale.

If an observation includes a sufficiently large number of patches, the resulting slope pdf will then follow a compound process according to the variability of the small-scale slope variance. The resulting slope pdf is non-Gaussian and written as

$$P(\mathbf{s}) = \int P(\mathbf{s}|\alpha) P(\alpha)\, d\alpha. \tag{3}$$

To illustrate such a development, we characterize the variability of the nonhomogeneous wave slope field by considering the following perturbation:

$$\alpha = \alpha_o(1 + \delta), \tag{4}$$

where δ represents a zero mean random fluctuation modulating the inverse of the overall mean slope variance, given as α_o for the remainder of this paper. As defined, (4) then represents a perturbation of the surface smoothness. Next, one can write

$$P(\mathbf{s}) = \int P[\mathbf{s}|\alpha(\delta)] P(\delta)\, d\delta$$

$$= \frac{\alpha_o}{\pi} \int (1 + \delta) e^{-\alpha_o(1+\delta)s^2} P(\delta)\, d\delta, \tag{5}$$

where $P(\delta)$ is the pdf associated with the random fluctuation δ. An expansion up to second order in δ then leads to

$$P(\mathbf{s}) = \frac{\alpha_o}{\pi} e^{-\alpha_o s^2} \int (1 + \delta) \cdot \left[1 - \alpha_o \delta s^2 + \frac{(\alpha_o \delta s^2)^2}{2} + \cdots \right] P(\delta)\, d\delta, \tag{6}$$

whence

$$P(\mathbf{s}) = \frac{\alpha_o}{\pi} e^{-\alpha_o s^2} \left[1 + \Delta\left(\frac{\alpha_o^2 s^4}{2} - \alpha_o s^2\right) + \cdots \right], \tag{7}$$

where Δ is defined to be the variance of the random fluctuation δ.

On comparison with the Gaussian definition (1) it is apparent that the randomness in slope variance modifies the shape of the resulting slope pdf. Taking the logarithm of this compound pdf and restricting the expansion to slope terms of the fourth power leads to the following development:

$$\ln P(\mathbf{s}) = \ln\left(\frac{\alpha_o}{\pi}\right) - \alpha_o s^2(1 + \Delta) + \frac{\alpha_o^2}{2} \Delta s^4 (1 - \Delta) + \cdots. \tag{8}$$

Evaluation of (8) at the lowest quadratic order indicates that the compound process model will lead to a change in the shape of the slope pdf near-zero slope. Here there will be an apparent increase of the inverse slope variance parameter by a factor $(1 + \Delta)$. The modified pdf will thus decrease more rapidly with measured slopes than for a Gaussian pdf; that is, the resulting compound pdf exhibits peakedness relative to a Gaussian distribution [e.g., *Jackson et al.*, 1992]. The positive peakedness is readily associated with the occurrence of an exceeding population of shallow slopes.

The higher fourth-order correction on the slope pdf will result in a slower than Gaussian decrease in population density for larger values in slope. This indicates that the occurrence of steep slope components is more probable in the compound process model than in the linear Gaussian case. It must be clear that the above expansion cannot be used for very steep slopes and that an extrapolation beyond a certain limit would be completely unrealistic. For extreme slope components, higher-order terms must be considered in (6) and (8). As a possible analytical illustrative solution, the fluctuations of the inverse slope variance can be chosen to follow a Gamma process with mean α_o and variance $\alpha_o^2(1 + \Delta)$, so that the resulting compound slope pdf is

$$P(s) = \frac{\alpha_0}{\pi}(1 + \alpha_o \Delta s^2)^{-(1+\Delta)/\Delta} \tag{9}$$

Taking the logarithm of this function and restricting the expansion to slope terms of the fourth power then gives:

$$\ln P(s) = \ln\left(\frac{\alpha_o}{\pi}\right) - \alpha_o s^2(1 + \Delta) + \frac{\alpha_o^2}{2}\Delta s^4(1 + \Delta) + \cdots \tag{10}$$

As compared with (8), a modification is introduced in the fourth-order term that comes from the omitted third-order moment of δ in (7). Indeed, the peak value of a Gamma distribution does not coincide with the value of its mean. However, to leading linear order in the Δ parameter the development remains consistent for both cases.

As presented, a compound process corresponds to the mixture of two random processes. It must be noted that the spatial and temporal correlations of the sea surface short wave slope components are usually assumed and observed to drop very rapidly with comparison to the longer gravity waves. The distinction in space and/or time of the slope wave field between two different scales can thus in general be readily made for the ocean surface. The physics of wave generation and interaction is not the same for long and short waves. Before breaking, short waves essentially grow under the direct energy input from the wind and the indirect straining effect of the longer waves. The lifetime for the short-scale waves that predominate inside a patch may thus be considered to be very short. This lifetime will certainly be much less than the necessary time of the nonlinear interactions among the short waves themselves, within a patch, that would lead to a permanent form such as a Stokes pattern. As already mentioned above, the smallest "large" scale corresponding to the introduction of the δ fluctuations can then be related to a fraction of the average wavelength and/or the period of the dominant surface waves. Other larger-scale sources of variability could also be included corresponding to scales representing mean wind gust spatial and temporal extent and/or dominant wave group length and duration. However, the choice of the exact form of the pdf for the fluctuations $(1 + \delta)$ is beyond the scope of this paper. Rather we wish to emphasize the compound process concept. Nevertheless, since the slope variance is a positive variable, the fluctuations must remain positive such as in the case of Rayleigh or Gamma random processes.

3. Cox and Munk Analysis

To date, and as systematically referenced when modeling the sea surface slope statistics, results derived from the glitter pattern of reflected sunlight photographed by Cox and Munk in 1951 remain the most reliable direct measurements of wind-dependent slope statistics. However, careful examination of their well-documented report [*Cox and Munk*, 1956] clearly shows that the statistical parameters presented by Cox and Munk are not directly computed from a measured slope pdf. Instead, they are inferred from the results of a fitting procedure and followed by a normalizing adjustment to compensate for what the Cox and Munk called the "incomplete" slope variances. Indeed, a lack of normalization for the probability distribution limited that study, leading the authors to consider only the best possible characterization of the shape (or falloff) of the logarithm of an unnormalized probability function as a function of wind speed. Documented measurement limitations dictated that the fitting procedure be limited to the smallest slopes (up to ~2.5 times the rms). Consequently, Cox and Munk could not directly provide the total slope variance but an estimate based on the shape analysis of the log of a truncated unnormalized slope pdf. As will be seen in section 5, their inferred measurement is directly analogous to near-nadir airborne altimeter backscatter measurements. Using a Gram-Charlier expansion to fourth order, their modeled fit was written as follows [*Cox and Munk*, 1956, equation (7.2-1)]

$$\begin{aligned}\ln P(s) = {} & a_o - a'_o s^2 + a''_o s^4 + s(a_1 - a'_1 s^2)\cos(\phi') \\ & + s^2(a_2 + a'_2 s^2)\cos(2\phi') + a_3 s^3 \cos(3\phi') \\ & + a_4 s^4 \cos(4\phi'),\end{aligned} \tag{11}$$

where ϕ' is the azimuthal angle according to principal axis and the coefficient a is defined as

$$a_o = \frac{1}{8}(c_{40} + c_{22} + c_{04}) - \ln(2\pi\sigma_c\sigma_u), \tag{12a}$$

$$a'_o = \frac{1}{4}\left(\frac{1}{\sigma_c^2} + \frac{1}{\sigma_u^2}\right) + \frac{1}{8}\left[\frac{c_{40}}{\sigma_c^2} + c_{22}\left(\frac{1}{\sigma_c^2} + \frac{1}{\sigma_u^2}\right) + \frac{c_{04}}{\sigma_u^2}\right], \tag{12b}$$

$$a''_o = \frac{1}{64}\left(\frac{c_{40}}{\sigma_c^4} + 2\frac{c_{22}}{\sigma_c^2\sigma_u^2} + \frac{c_{04}}{\sigma_u^4}\right), \tag{12c}$$

$$a_1 = \frac{c_{03} + c_{21}}{2\sigma_u}, \tag{12d}$$

$$a'_1 = \frac{1}{8\sigma_u}\left(\frac{c_{21}}{\sigma_c^2} + \frac{c_{03}}{\sigma_u^2}\right), \tag{12e}$$

$$a_2 = \frac{1}{4}\left(\frac{1}{\sigma_c^2} - \frac{1}{\sigma_u^2}\right) + \frac{1}{8}\left[\frac{c_{40}}{c\sigma_c^2} + c_{22}\left(\frac{1}{\sigma_c^2} - \frac{1}{\sigma_u^2}\right) + \frac{c_{04}}{\sigma_u^2}\right], \tag{12f}$$

$$a'_2 = \frac{1}{4}\left(\frac{c_{40}}{\sigma_c^2} - \frac{c_{04}}{\sigma_u^2}\right), \tag{12g}$$

$$a_3 = \frac{1}{8\sigma_u}\left(\frac{c_{21}}{\sigma_c^2} - \frac{c_{03}}{3\sigma_u^2}\right), \tag{12h}$$

$$a_4 = \frac{1}{192}\left(\frac{c_{40}}{\sigma_c^4} - 6\,\frac{c_{22}}{\sigma_c^2\sigma_u^2} + \frac{c_{04}}{\sigma_u^4}\right), \tag{12i}$$

where σ_c and σ_u are the rms slope components along the principal axes and c_{ij} are the expansion coefficients related to the cumulants of the slope distribution.

Distribution skewness to first order vanishes when considering the omnidirectional isotropic case where $\sigma_c = \sigma_u$ (see the appendix for a two-dimensional development). Equation (11) then reduces to

$$\ln P(s) = a_o - a'_o s^2 + a''_o s^4. \tag{13}$$

Equation (13) is obviously congruent with the compound process development given as (8) or (10). By identification, it follows that for both cases

$$a'_o = \alpha_o(1 + \Delta). \tag{14}$$

Thus when applied to the logarithm of a pdf, both the Gram-Charlier expansion of Cox and Munk and our compound model can lead to an estimate of the mean square slope ($\mathrm{mss}_o = 1/\alpha_o$) that is based on an estimate of the lowest-order fit parameter modified by a higher-order correction such that

$$\mathrm{mss}_o = \frac{1}{\alpha_o} = \frac{1 + \Delta}{a'_o}. \tag{15}$$

In this case, a'_o is used to remain consistent with Cox and Munk's nomenclature.

The correction coefficient $(1 + \Delta)$ in (15) is equivalent to Cox and Munk's noted constant adjustment factor to arrive at their often cited total mean square slope model. Their correction term multiplies their inference of an "incomplete" slope variance $1/a'_o$ to account for infrequent and unmeasured steep slopes [see *Cox and Munk*, 1956, sections 7.3 and 9]. Following a compound process interpretation, the correction becomes a measure of the overall randomness of the surface slope wave field. For this model, steep slopes will be locally associated with an enhanced variance parameter, i.e., small α values. However, as expected for a random ocean surface, large slope components will likely be followed by smaller slopes, i.e., large α values. Thus high roughness areas correspond to calm areas. This is statistically characterized by the fluctuation-normalized variance Δ in the compound model.

For Cox and Munk the proposed correction factor is deemed independent of wind speed and is nearly identical for the principal wind direction axes. The factor does not vary much with the change between clean and slick (attenuated small-scale waves) surface conditions. Their analysis derives a value of ~1.23 ($\Delta = 0.23$) that is valid for their whole clean surface data set and 1.20 for the case of measurements over a slick surface. Note that if one chose a Rayleigh distribution to describe the random fluctuations, Δ is a constant equal to $(4/\pi - 1) \simeq 0.27$.

Conclusions from this examination are summarized as follows. First, when inferring parameters from a fit to the log of the pdf, it is clear that the most direct of comparison to the Cox and Munk results is through their fit parameters [e.g., *Shaw and Churnside*, 1997] and not their reported total slope variance model. Second, the proposed correction to account for steep waves (or pdf peakedness) is nearly 25%. This is a substantial correction to a Gaussian assumption and not without its skeptics [e.g., *Wentz*, 1976]. While Cox and Munk suggest that the correction is a constant (i.e., independent of wind speed, sea state, etc.), their inability actually to measure the steep slopes would suggest that alternate measurements to clarify variability and magnitude would be beneficial. Finally, although this correction factor is of crucial importance for precise inference of the mean variance mss_o, the foremost physically relevant result is perhaps not the correction's value but the simple fact that its existence indicates multiple scales of variability over a surface slope wave field.

4. Wave-Breaking Statistics Under a Compound Process

An attractive feature of the compound model is that it leads to a fairly simple mathematical expansion describing complex statistical processes at the surface. The following discussion uses this aspect to address a possible relationship between the compound slope pdf and wave breaking statistics.

Following Gaussian statistical assumptions, *Srokosz* [1986] used the extension of earlier statistical models for the distribution of maxima of a random surface [*Cartwright and Longuet-Higgins*, 1956] to derive a wave-breaking probability density P_b based upon the likelihood that slopes at the wave crests exceed a given critical slope value:

$$P_b = e^{-(1/2)\gamma^2\alpha}, \tag{16}$$

where α is the inverse slope variance and γ is the threshold criterion associated with the critical slope. Conceptually, this value is related to the ratio between the downward acceleration and the restoring acceleration (including gravitational and surface tension effects).

Following a compound process approach, it is possible to extend this breaking probability model to a random nonstationary wave field. As for the sea surface slope pdf development, we consider that a Gaussian assumption may locally apply, with random fluctuations characterized by $\alpha_o(1 + \delta)$, so that the resulting compound-breaking probability becomes

$$P_b = e^{-(1/2)\gamma^2\alpha_o}\left[1 + \frac{\Delta}{2}\left(\frac{\gamma^2\alpha_o}{2}\right)^2 + \cdots\right], \tag{17}$$

where we only considered an expansion up to second order in δ with variance Δ.

Thus, at this lowest order a correction term is again simply introduced to integrate some nonhomogeneous characteristics of the surface wave field. This indicates that the correction term is first characterized by the variance Δ of the inverse slope parameter fluctuations. As obtained, the breaking probability increases when the randomness of the wave field is included. The ratio between breaking probability models, compound and linear, will also decrease toward unity with wind speed since α_o decreases with wind speed. As should be expected, a Gaussian model should hold for the highest wind speeds. For completeness the breaking probability can be derived for the case of random Gamma-distributed fluctuations. As for the pdf, an analytical solution can be found:

$$P_b = \left(1 + \frac{\alpha_o\Delta\gamma^2}{2}\right)^{-1/\Delta}. \tag{18}$$

Using the results derived from Cox and Munk's reported fit coefficients, the compound breaking probability obtained for a threshold value $\gamma = \tan 22° \simeq 0.4$ is given in Figure 1. According to our reinterpretation of *Cox and Munk*'s [1956] results the density of short steep wavelets grows more rapidly at lower wind speed than it does for a Gaussian prediction. The Gaussian model (squares) is always lower than the compound model (stars). Moreover, the compound breaking seems to occur sooner than that of the Gaussian. Both models, however, converge at high wind speeds. For indication the breaking density for the compound model is almost quadratic in wind speed.

5. Application to Altimeter Ocean Backscatter Models

The most common model of microwave backscatter from ocean surfaces at normal and near-nadir incidences is the specular point model [*Brown*, 1978]. Thus, in their physical and practical applications, altimeter techniques rely heavily on the definition of the slope pdf and its change versus wind speed or friction velocity.

5.1. Inferring PDF Shape With Airborne Near-Nadir Measurements

As thoroughly described by *Walsh et al.* [1998], one aircraft technique for determining a radar-inferred mean square slope parameter is to use the relative variation of the backscatter power measured with respect to incidence angle [see also *Jackson et al.*, 1992; *Vandemark et al.*, 1994]. Indeed, assuming that a specular point model may be applicable to describing the radar sea surface scattering mechanism out to an incidence angle of about $\theta = 12°$, the decrease in the radar backscatter coefficient $\sigma_0(\theta)$ with angle for an isotropic surface would be proportional to the slope pdf, such as

$$\sigma_0(\theta) \propto \sec^4 P(\tan \theta). \qquad (19)$$

After correction for the $\cos^4 \theta$ dependence this type of near-nadir measurement should be analogous to optically derived results of *Cox and Munk* [1956]. Results to date from such systems have made use of only the simple parabolic approximation leading to a simple parameter estimation, the so-called fit or shape mean square slope parameter [e.g., *Jackson et al.*, 1992]. This parameter is regarded, under assumed Gaussianity, as a radar inference of the total mean square slope with any difference between the reported total value of Cox and Munk attributed to a radar's implicit low-pass filtering of short-scale slopes. Ku band and Ka band radar-derived mean square slope estimates appear to agree fairly well with optical prediction in their overall increase with wind speed, but differences do appear such as radar mean square slope nonlinearity over the complete wind speed range and an absolute overall difference between reported values, the radar being significantly lower.

As already anticipated by *Jackson et al.* [1992] with a suggested 6% increase for surface peakedness, it is clear from the slope pdf developments presented in sections 2 and 3 that a parabolic approximation may not be sufficient to retrieve a precise estimate of the slope variance. Following the formulation given by (8), a more general approximation of the quasi-specular radar backscatter becomes

$$\ln[\sigma^o(\theta)\cdot\cos^4\theta] = \text{const} - \alpha_o(1+\Delta)\tan^2\theta \cdot\left(1 - \alpha_o\Delta\frac{1-\Delta}{1+\Delta}\tan^2\theta\right). \qquad (20)$$

In past radar studies the incidence angle fit window has been taken to be wind independent and set between $0 \leq \tan\theta \leq \tan\theta_{max}$. As seen above, the parabolic approximation term now depends upon the values of both Δ and $\alpha_o \tan^2\theta$ over the

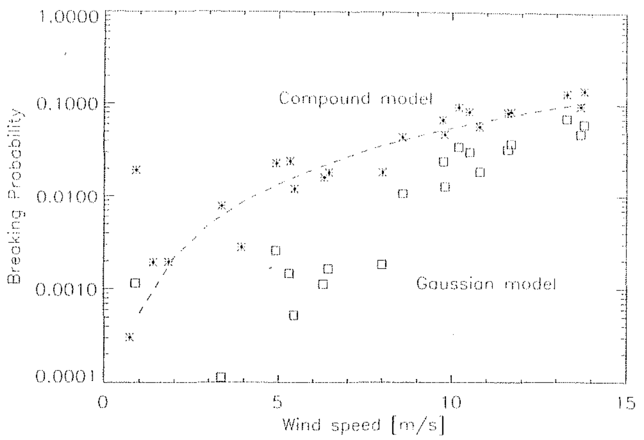

Figure 1. Wave-breaking probability as inferred from reported fit coefficients by *Cox and Munk* [1954] when imposing a threshold value $\gamma = \tan 22° \simeq 0.4$. The Gaussian model (squares) is always lower than the compound model (stars). The dashed curve is a parabolic fit to the compound breaking model ($5.5\ 10^{-4}\ U_{10}^2$). Some squares of the Gaussian model fall bellow the minimum line at 10^{-4} and therefore do not appear on the plot.

range of incidence angles used to define the fit window. Taking Δ as approximately constant, the goodness of the fit will still be wind dependent since α_o is wind dependent. As the wind speed increases, α_o is expected to decrease so that the quadratic correction term may be neglected within the fit window. In this special case (near-zero slope) the modeled slope distribution peakedness will result in a correction to the "total" radar mean square slope under a Gaussian assumption of $1/(1 + \Delta)$. In effect past data sets may have been underestimating the radar-inferred mean square slope.

Under light wind conditions, α_o becomes quite large, and the quadratic correction may not be totally neglected over the fit window. For such cases a parabolic fit will lead to estimates of radar shape mean square slope parameters closer to the total mean square slope parameters. As perfectly illustrated by *Walsh et al.* [1998, Figure 12], the shape parameter will then be highly dependent upon the incidence angle limit θ_{max} taken for the fit window. We also point out that the parabolic fit coefficient in (20) will decrease as the $\alpha_o \tan^2\theta$ correction term becomes predominant. As is also shown by *Walsh et al.* [1998] and already discussed, the higher the slope variance (increasing wind speed), the less sensitive the measurement technique using a parabolic approximation for the slope pdf.

Under (20), comparisons between near-nadir radar estimates and Cox and Munk's reported parameters should be more straightforward. For intermediate to high wind speeds the analysis suggests that it is more judicious to compare Cox and Munk's optical measurements and radar results only in terms of their parabolic approximation parameters a'_o.

Figure 2 presents the different shape-based second-order regression estimates as reported by *Cox and Munk* [1956] and *Jackson et al.* [1992] for a Ku band radar instrument and *Walsh et al.* [1998] for a Ka band radar instrument. As shown, an overall close agreement is found between optical- and radar-inferred parameters. This suggests that a Ku band instrument (~2 cm wavelength) and, moreover, a Ka band instrument (0.8 cm wavelength) almost entirely probe the total sea surface roughness. The comparison shows that the shape parameter at

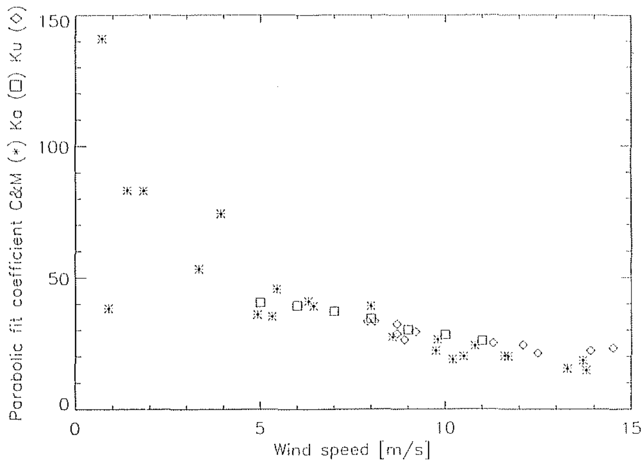

Figure 2. Second-order regressions of the shape-based parameter as reported by *Cox and Munk* [1956] (stars), *Jackson et al.* [1992] (squares), and *Walsh et al.* [1998] (diamonds) for optical, Ku band, and Ka band, respectively. All sources are in near agreement for winds ranging from 5 to 11 m s^{-1}.

14 Ghz (Ku band) is only departing from the optical Cox and Munk's reported parameter for the highest wind speed conditions, $U_{10} \geq 10$ m s^{-1}. We suggest that future effort be made to validate radar inference of the Cox and Munk adjustment for the incomplete variance by a full evaluation using (20).

5.2. Effect at Normal Incidence

The application of these concepts to the satellite altimeter (e.g., Geosat or TOPEX) comes for the case of a viewing geometry extremely near the vertical, perhaps no more than 0.1°–0.2° from nadir incidence. Again, following the specular point theory for altimeter backscatter, we simply have at nadir

$$\sigma^o(0^o) = \pi R^2 P(\mathbf{0}), \tag{21}$$

with R^2 denoting the Fresnel power reflection coefficient for a flat sea surface. If the definition of the slope pdf is given by the compound model expansion, we then have

$$\sigma^o(0^o) = \alpha_o R^2. \tag{22}$$

As shown earlier, the wind speed–dependent α_o parameter is not correctly retrieved from a single-parameter second-order shape analysis. However, in the range of moderate to high wind speed the inverse slope variance may well be approximated using the shape-based parabolic regression estimate and an adjustment factor $(1 + \Delta)$, leading to

$$\sigma^o(0^o) = \frac{a'_o R^2}{1 + \Delta} = a'_o R^2_{\mathrm{eff}}, \tag{23}$$

where we introduce an effective Fresnel coefficient, R_{eff}, as is common practice when comparing airborne and satellite-borne altimeter data. In past studies [e.g., *Masuko et al.*, 1986; *Jackson et al.*, 1992; *Wu*, 1994] this factor is a catch-all adjustment (typically a constant) to carry various possible uncertainties. These uncertainties have included calibration problems, possible errors in Fresnel coefficient values, and varied definitions of radar scattering or surface description assumptions. As is obvious from (23), we suggest that it may actually be dominated by a peakedness correction. The nominal Fresnel power coefficient for seawater is $R^2 \simeq 0.6$ at Ku band. The total expected variation is ~0.3 dbar for extreme variations in water temperature and salinity. If we assume that optical estimates apply to Ku band altimeter data, the measurements reported by Cox and Munk could lead to much greater changes with a proportionality constant ranging from 1 to 0.6 to give an effective Fresnel coefficient between 0.6 and 0.36. For the average constant correction adopted by Cox and Munk, $\Delta \simeq 0.25$, the nadir correction is 0.8 to give an effective Fresnel coefficient of 0.48. At the present time the best estimate of the effective Fresnel coefficient for a Ku-band system comes from the absolutely calibrated TOPEX radar cross section data [*Archiving, Validation and Interpretation of Satellite Oceanographic Data (AVISO)*, 1992; *Benada*, 1997]. This system has a documented signal difference of .85 dB above the Geosat altimeter [*Callahan et al.*, 1994]. Combining results of *Jackson et al.* [1992] with this information leads to a present estimate of 0.45 for the effective Fresnel coefficient at Ku band and wind speeds between 7 and 14 m s^{-1}. Following this development it seems that most of the discrepancy between the nominal and effective Fresnel coefficient is explained by considering the peakedness correction based on Cox and Munk's incomplete variance adjustment.

6. Summary and Conclusion

The shape of the ocean slope pdf will exhibit peakedness relative to a Gaussian distribution by introducing randomness in the surface slope variance to characterize nonstationarities in the surface wave field. This indicates that the occurrence of small and steep slopes is more probable than under a Gaussian assumption. Such a development is congruent with the analysis used by Cox and Munk to interpret the statistics of measured sunlight glitter patterns. In particular, the slope variance parameters provided by Cox and Munk and commonly used in the literature were not directly measured from the optical data but inferred from the results of a fitting procedure followed by a "blanket increase" to take into account the lack of information concerning very infrequent, very large slopes. From our proposed analysis the necessary adjustment is directly related to the variance parameter associated with the overall variability of the surface slope wave field. Wave-breaking statistics have also been predicted on the basis of this compound process model. In such a case the breaking probability can also be derived from the probability that the slope crosses a given level at the wave crests. On the basis of Cox and Munk's analysis and results, it is then found that for a given threshold criterion the short-scale breaking probability under a compound process assumption will be increased.

On the basis of the assumption that the specular point model is applicable to describe near-nadir Ku band and Ka band radar sea surface backscatter measurements we further showed that an unmodeled slope distribution peakedness will usually lead to an underestimation of the total radar-inferred mean square slope. The goodness of the simplified parabolic approximation over a fixed fit window will then be wind dependent based on the slope variance values. As the wind speed increases, the parabolic approximation may be sufficient to lead to a correction similar to the one used by Cox and Munk to compare the incomplete variance (shape mean square slope) with the total variance. By comparing both the optical and the radar shape mean square slopes we further found that radar estimates are on average only 15% below optical results for moderate to high wind speed conditions. Moreover, the peakedness correction has also been shown to help to explain most of the necessary adjustment needed to compare airborne and satellite-borne altimeter measurements. On the basis of the correction value introduced by Cox and Munk the effective Fresnel coefficient at Ku band may be lowered to ~0.48. This compares well to those effective Fresnel coefficients predicted from the TOPEX altimeter [see *Jackson et al.*, 1992].

To conclude, it appears that if we are to gain information on the statistical description of the sea surface geometry, we can certainly rely on high-frequency radar measurements at near-nadir incidence angles but with an improved fit procedure as suggested by Cox and Munk to include the fourth-order correction. Further, it seems to be of particular interest to refine analysis and measurement techniques used to resolve peakedness and its association with an overall variability of the wave field caused by environmental conditions (wind speed, stability, swell, current, etc.). Results of such investigations should directly improve the physical interpretation of nadir and off-nadir remote sensing measurements. In addition, these data and concepts are applicable to the determination of wave-breaking statistics and may provide a better quantification of gas transfer processes at the sea surface.

Appendix: Directional Aspect

The local Gaussian pdf is defined as

$$P(s_x, s_y) = \frac{\alpha_x\alpha_y}{2\pi} e^{-(1/2)[(\alpha_x s_x)^2+(\alpha_y s_y)^2]}. \tag{A1}$$

As defined for the omnidirectional case, the compound process is introduced by considering some random fluctuations for both α_x^2 and α_y^2 around their mean values α_{ox}^2 and α_{oy}^2, respectively. Following this development, the normalized variances of the fluctuations in upwind and cross-wind directions are equal to Δ. Following such an assumption, the resulting expansion of the logarithm of the compound pdf is given by

$$\begin{aligned}\ln P(s_x, s_y) &= \ln\left(\frac{\alpha_{ox}\alpha_{oy}}{2\pi}\right) - \frac{\alpha_{ox}^2}{2} s_x^2(1+\Delta) - \frac{\alpha_{oy}^2}{2} s_y^2(1+\Delta) \\ &+ \frac{\alpha_{ox}^4}{8}\Delta s_x^4(1-\Delta) + \frac{\alpha_{oy}^4}{8}\Delta s_y^4(1-\Delta) \\ &+ \frac{\alpha_{ox}^2\alpha_{oy}^2}{4}\Delta s_x^2 s_y^2(1-\Delta) \ldots .\end{aligned} \tag{A2}$$

We then develop the slope components as

$$s_x s \cos\phi \text{ and } s_y = s \sin\phi \tag{A3}$$

to obtain

$$\begin{aligned}\ln P(s) &= \ln\left(\frac{\alpha o_{ox}\alpha_{oy}}{2\pi}\right) - \frac{s^2}{4}(\alpha_{ox}^2 + \alpha_{oy}^2)(1+\Delta) \\ &+ \frac{s^4}{64}(2\alpha_{ox}^4 + 2\alpha_{oy}^4 + (\alpha_{ox}^2+\alpha_{oy}^2)^2)\Delta(1-\Delta) \\ &+ \frac{s^2}{4}\left[(\alpha_{oy}^2 - \alpha_{ox}^2)(1+\Delta)\right. \\ &\left. + \frac{s^2}{4}(\alpha_{ox}^4 - \alpha_{oy}^4)\Delta(1-\Delta)\right]\cos 2\phi \\ &+ \frac{s^4}{64}(\alpha_{ox}^2 - \alpha_{oy}^2)^2\Delta(1-\Delta)\cos 4\phi.\end{aligned} \tag{A4}$$

After direct identification with Cox and Munk's modeled fit (11) we determine the ratio between upwind and cross-wind local slope variances as

$$\beta = \frac{\alpha_{ox}^2}{\alpha_{oy}^2} = \frac{\mathrm{mss}_{oy}}{\mathrm{mss}_{ox}} = \frac{a'_o - a_2}{a'_o + a_2} \tag{A5}$$

It must be noted that it is also possible to determine this ratio from

$$\beta = \frac{4a''_o 3a'_2}{4a''_o - 1}, \tag{A6}$$

which is only associated with fourth-order slope terms in the expansion. Cox and Munk found the a'_2 coefficients to be mostly negative. This result indicates that $\beta < 1$ as expected but also that the slope pdf exhibits peakedness in both upwind and cross-wind directions.

Following the Gaussian assumption on a local patch, the relationship for the mean slope variance is

$$\mathrm{mss}_o = \frac{1}{\alpha_o^2} = \frac{1}{\alpha_{ox}^2} + \frac{1}{\alpha_{oy}^2}, \tag{A7}$$

leading to the direct evaluation from Cox and Munk's a'_o reported fit coefficients

$$\mathrm{mss}_o = \frac{(1+\beta)^2(1+\Delta)}{4\beta a'_o}. \tag{A8}$$

To determine Δ, the following relationship can be used:

$$\frac{\Delta(1-\Delta)}{(1+\Delta)^2} = \frac{4(1+\beta)a''_o}{(3+\beta)a'^2_o}. \tag{A9}$$

As developed, the introduction of directionality, i.e., $\beta < 1$, will impact the value of Δ as compared to the omnidirectional case. The correction $(1 + \Delta)$ will be slightly lowered by the factor $(1 + \beta)^2/(4\beta)$. Keeping Cox and Munk's reported fit parameters that satisfy $a''_o \neq 0$ and $a_2 > 0$, the ratio between cross-wind and upwind slope variances is almost constant over the wind speed range with a mean value $\beta \simeq 0.65$. With this value the correction $(1 + \Delta)$ is approximately lowered by 0.95 as compared to the isotropic case.

References

Archiving, Validation and Interpretation of Satellite Oceanographic Data (AVISO), User's handbook: Merged TOPEX/poseidon products, *Tech. Rep. AVI-NT-02-101-CN*, Toulouse, France, 1992.

Benada, J., Merged gdr (TOPEX/Poseidon), in *User's Handbook Version 2.0* [CD-ROM], Jet Propul. Lab., Pasadena, Calif., 1997.

Brown, G., Backscattering from a Gaussian distributed perfectly conducting rough surface, *IEEE Trans. Antennas Propag.*, *26*, 472–482, 1978.

Callahan, P., C. Morris, and S. Hsiao, Comparison of TOPEX/Poseidon σ^o and significant wave height distributions to Geosat, *J. Geophys. Res.*, *99*, 25,015–25,024, 1994.

Cartwright, D., and M. S. Longuet-Higgins, The statistical distribution of the maxima of a random function, *Proc. R. Soc. London, Ser. A*, *237*, 212–232, 1956.

Cox, C., and W. Munk, Statistics of the sea surface derived from Sun glitter, *J. Mar. Res.*, *13*, 198–227, 1954.

Cox, C., and W. Munk, *Slopes of the Sea Surface Deduced From Photographs of Sun Glitter*, Univ. of Calif. Press, Berkeley, 1956.

Gotwols, B. L., and D. R. Thompson, Ocean microwave backscatter distributions, *J. Geophys. Res.*, *99*, 9741–9750, 1994.

Jackson, F., W. Walton, B. Walter, and G. Peng, Sea surface mean square slope from ku-band backscatter data, *J. Geophys. Res.*, *97*, 11,411–11,427, 1992.

Longuet-Higgins, M. S., The effects of non-linearities on statistical distribution in the theory of sea waves, *J. Fluid Mech.*, *17*, 459–480, 1963.

Longuet-Higgins, M. S., On the skewness of sea-surface slopes, *J. Phys. Oceanogr.*, *12*, 1283–1291, 1982.

Masuko, H. K., M. Shimada, and S. Niwa, Measurements of microwave backscattering signatures of the ocean using x-band and ka-band airborne scatterometers, *J. Geophys. Res.*, *91*, 13,065–13,083, 1986.

Plant, W. J., A two-scale model of short wind-generated waves and scatterometry, *J. Geophys. Res.*, *91*, 10,735–10,749, 1986.

Shaw, J., and J. Churnside, Scanning laser glint measurements of sea-surface slope statistics, *Appl. Opt.*, *36*, 4202–4213, 1997.

Srokosz, M., On the probability of wave breaking in deep water, *J. Phys. Oceanogr.*, *16*, 382–385, 1986.

Valenzuela, G. R., Theories for the interaction of electromagnetic and oceanic waves: A review, *Boundary Layer Meteorol.*, *13*, 61–85, 1978.

Vandemark, D., F. Jackson, E. Walsh, and B. Chapron, Airborne radar measurements of ocean wave spectra and wind speed during the grand banks ERS-1 SAR wave experiment, *Atmos. Ocean*, *32*, 143–178, 1994.

Vandemark, D., J. Edson, and B. Chapron, Altimeter estimation of sea surface wind stress for light to moderate winds, *J. Atmos. Oceanic Technol.*, *14*, 716–722, 1997.

Walsh, E., D. Vandemark, C. Friehe, S. Burns, and D. Khelif, Measuring sea surface mean square slope with a 36-GHz scanning radar altimeter, *J. Geophys. Res.*, *103*, 12,613–12,628, 1998.

Wentz, F., Cox and Munk's sea surface slope variance, *J. Geophys. Res.*, *81*, 1607–1608, 1976.

Wu, J., Microwave specular reflections from sea surface: A continuous altimeter-wind algorithm from breeze to hyrricane, paper presented at 2nd International Conference on Air-Sea Interaction and on Meteorology and Oceanography of the Coastal Zone, Am. Meteorol. Soc., Lisbon, Portugal, 1994.

B. Chapron and V. Kerbaol, Département d'Océanographie Spatiale, IFREMER, centre de Brest, BP 70, 29280 Plouzané, France.

T. Elfouhaily, Applied Physics Laboratory, Johns Hopkins University, 11100 Johns Hopkins Road, Laurel, MD 20723-6099. (Elfouhaily@jhuapl.edu)

D. Vandemark, Laboratory for Hydrospheric Processes, NASA Goddard Space Flight Center, Wallops Island, VA 23337.

(Received March 9, 1999; revised April 13, 2000;
accepted April 14, 2000.)